Dynamic–Analogue Correction of the Decadal Change of East Asian Summer Precipitation in the Late 1990s

GONG Zhiqiang[1*] (龚志强), LI Shangfeng[2] (李尚峰), HU Po[3] (胡 泊), SHEN Baizhu[2] (沈柏竹), and FENG Guolin[1,2] (封国林)

1 *Laboratory for Climate Studies and Climate Prediction, National Climate Center, China Meteorological Administration, Beijing* 100081

2 *Laboratory of Research for Middle-High Latitude Circulation and East Asian Monsoon, Jilin Meteorological Science Institute, Changchun* 130062

3 *Department of Physics, Yangzhou University, Yangzhou* 225009

(Received November 15, 2015; in final form March 18, 2016)

ABSTRACT

This paper systematically evaluates the deviations that appear in the hindcasts of the East Asian summer precipitation (EASP) decadal change in the late 1990s in two global coupled models (BCC_CGCM and BCC_CSM). The possible causes for the deviations between the model hindcasts and observations are analyzed. The results show that the hindcasts of EASP by BCC_CGCM and BCC_CSM deviate from observations, with the anomaly correlation coefficient (ACC) being –0.01 and –0.09 for the two models, respectively. The SST anomalies in North and West Pacific and the SST index values predicted by the two models also deviate from the observations, indicating that inconsistent SST fields may be the key factor leading to the deviation in the prediction of the EASP decadal shift. Thus, a dynamic-analogue scheme is proposed to correct the precipitation hindcasts by using SSTs, where SST and EASP are highly correlated, to select historical analogue cases. Cross validations show that the average ACC of the temporal-latitude distribution of the EASP between the corrected hindcasts and observations is 0.18 for BCC_CGCM and 0.02 for BCC_CSM; both are much higher than the uncorrected hindcasts. Applying the dynamic-analogue correction scheme in both models successfully improves prediction of the EASP decadal change in the late 1990s.

Key words: dynamic–analogue correction scheme, East Asian summer precipitation, ocean-atmosphere coupled model, decadal change

Citation: Gong Zhiqiang, Li Shangfeng, Hu Po, et al., 2016: Dynamic–analogue correction of the decadal change of East Asian summer precipitation in the late 1990s. *J. Meteor. Res.*, **30**(3), 341–355, doi: 10.1007/s13351-016-5220-1.

1. Introduction

Under the combined effects of natural and human variability, the East Asian summer precipitation (EASP) shows obvious decadal variation characteristics (Chen et al., 1992; Ding, 1992; Huang and Yan, 1999). In the past five decades, EASP has undergone obvious decadal change in the late 1970s and early and late 1990s (Wang, 2001; Ding et al., 2008; Zhou et al., 2009; Huang et al., 2011). During 1993–1998, the summer precipitation anomaly in eastern China presented meridionally a "+ − +" tripole pattern as well as a "+ −" dipole pattern, while later it showed only the "+ −" dipole (i.e., "southern flood and northern drought") pattern during 1999–2009 (Huang et al., 2011). Gong et al. (2013) reported that after experiencing a wet period in the early 1990s, the Northeast Asian summer precipitation had been consistently reduced since the late 1990s; however, two consecutive years of anomalously wet conditions occurred in 2011

Supported by the National Natural Science Foundation of China (41575082 and 41305075), China Meteorological Administration Special Public Welfare Research Fund (GYHY201306021), and National Basic Research and Development (973) Program of China (2012CB955203).

*Corresponding author: gongzq@cma.gov.cn.

©The Chinese Meteorological Society and Springer-Verlag Berlin Heidelberg 2016

and 2012, and summer precipitation in far eastern areas of Russia and Northeast China continued to increase in 2013. Therefore, a decadal shift of precipitation anomaly from negative to positive occurred in the late 1990s, and an investigation on this decadal shift of summer precipitation in East Asia, especially over the mid–high latitudes, is necessary.

As an important part of the air-sea systems in the mid–high latitudes, North Pacific is located in the downstream area of Eurasia, where the sea and land show inhomogeneity in atmospheric heating on the decadal scale, creating favorable thermodynamic conditions for anomalies in the East Asian subtropical circulation system (Ding, 1992; Lian et al., 2003, 2004). For example, as the main mode of the monthly average SST to the north of 20°N in the Pacific, the Pacific Decadal Oscillation (PDO) reflects long-term El Niño-type Pacific climate variability (Bond and Harrison, 2000), in response to the influences of ENSO on the subtropical climate, through changing the background field of the decadal-scale average flow corresponding to various teleconnections (Gershunov and Barnett, 1998; Huang et al., 1998; Wang et al., 2008). Yang et al. (2005) and Ma and Fu (2007) revealed that the weakening of the East Asian summer monsoon (EASM) has an important relationship with the change in the North Pacific PDO. In addition, as the main mode of alternated cold–warm phase changes in the Atlantic SST (Enfield et al., 2001), the Atlantic Multidecadal Oscillation (AMO) exerts important effects on Eurasian summer climate. Ma and Fu (2007) proposed that the AMO is a major cause of the decadal change in the summer precipitation of North China, manifested as the positive phase of the AMO favoring increased summer precipitation over this region. Wu et al. (2003) proved that the summer tripole SST anomaly in North Atlantic could activate the Atlantic–Eurasian teleconnection in the mid–high latitudes, modulate the blocking highs over the Ural Mountains and the Sea of Okhotsk, and affect the zonal water vapor transport from west to east. Xu et al. (2013) put forward that the tripole structure of the North Atlantic SST can influence the precipitation anomaly in the following season over north-central East Asia by the interaction between the so-called "atmospheric bridge" and "ocean bridge."

Xu et al. (2015) found that the decadal shift in China's summer precipitation in the late 1990s shows certain characteristics in its spatial distribution; specifically, the decadal shift seems to propagate from northeast to southwest, i.e., it is mainly in the east around 1999, and then concentrated in the southwest in 2002/2003. The former was largely influenced by the PDO, while the latter was affected by the North Atlantic SST warming. It has been recognized that decadal anomalies of the atmosphere–ocean system in the mid–high latitudes, such as in North Pacific and West Pacific, are bound to have important influences on climate variability in East Asia. To improve the corresponding model prediction, the role of North Pacific and West Pacific SSTs has to be focused on.

Decadal-scale climate prediction research aims to improve a model's skill in predicting future climate change. Indeed, a large body of research exists regarding the improvement of SST prediction (Smith et al., 2007; Keenlyside et al., 2008), but credible decadal background information for seasonal climate prediction needs to be provided as well. In other words, how to increase the amount of decadal change information contained within the seasonal prediction results is an issue deserving of attention. However, the ability of most models to predict interannual and decadal climate variables is poor, leading to uncertainty in terms of their application (He et al., 2012; Kim et al., 2012; Wang et al., 2012).

The development of coupled climate dynamic models such as BCC_CGCM (Ding et al., 2002; Li et al., 2005) and BCC_CSM (Wu et al., 2013) has improved China's ability to make seasonal climate prediction. On the seasonal timescale, climate is the result of the interaction between seasonal- and decadal-scale variability. Considering the low skill of dynamical models in terms of their corresponding decadal-scale adjustment of basic climate elements (Smith et al., 2013), especially precipitation, how to effectively improve the decadal change information contained within a model's seasonal prediction currently remains a problem in climatological studies.

To improve the accuracy of climate prediction, the feasibility to combine dynamical and statistical information in short-term climate prediction was discussed by Chou (1974). By effectively using the correlation between a model's seasonal precipitation prediction errors and the precursory large-scale anomalies, such as those of circulation, snow cover, and SST, several dynamic–analogue correction methods have been proposed; for example, the evolutionary analogue-based multi-time prediction method (Chou, 1986; Huang et al., 1993) and the atmosphere self-memorization-based prediction method (Feng et al., 2001, 2013). In recent years, a series of new dynamic–analogue correction schemes have been developed and used in operational forecasting (Zheng et al., 2009; Wang et al. 2012), such as in precipitation forecasts for the Yangtze River basin region (Wang et al., 2011; Gong et al., 2012) and North China (Yang et al., 2012). Meanwhile, research on precipitation forecasts in a specific season such as autumn, winter, and spring (Lang and Wang, 2010), as well as prediction of the EASP using the interannual increment prediction method (Fan et al., 2007), has also been undertaken. Based on a dynamic–analogue correction method, Gong et al. (2013, 2015) explored the possibility to increase the amount of decadal change information within seasonal forecast results.

On the basis of the above context, the present paper evaluates the decadal change information related to the EASP in the late 1990s contained within the hindcasts of BCC_CGCM for about 30 years (1983–2011) and BCC_CSM for 20 years (1991–2011). The SST forecasting skill and the correlation between SST indexes and EASP in the model hindcasts are analyzed. The possible causes of the deviation in the decadal change of EASP in the model hindcasts are then investigated. Finally, a dynamic–analogue correction scheme for improving the EASP decadal change in the models' seasonal prediction is proposed, and cross sample validation is performed to demonstrate the effectiveness of the proposed scheme.

2. Data

BCC_CGCM refers to the National Climate Center/IAP T63 atmosphere-ocean coupled model, with a horizontal resolution of 1.875° × 1.875° and 30 layers in the vertical, performing ensemble seasonal forecast with 48 members (Ding et al., 2002; Li et al., 2005). The results from the hindcast for the years before 2005 and the operational prediction for 2005 and later, generated by BCC_CGCM, cover the period 1983–2011 and are interpolated onto 2.5° × 2.5° grids. The hindcast and prediction results are briefly termed as hindcasts below. The average yearly anomaly correlation coefficient (ACC) of precipitation between BCC_CGCM and observation is 0.01 and –0.01 before and after 2005, respectively. Similar average ACCs indicate that the forecast skill is very close to that of hindcasts, reflecting the possibility of integrating hindcasts and forecasts. Besides, the purpose of this paper is to investigate the decadal change of precipitation around 1999 and improve the decadal change information contained within the model output, which also requires an integrated hindcast and prediction dataset.

BCC_CSM is a global ocean–land–ice–atmosphere coupled climate system model, with a horizontal resolution of nearly 110 km (Wu et al., 2013), carrying out ensemble seasonal forecast with 24 members. The hindcasts generated by BCC_CSM cover the period 1991–2011, and are interpolated onto 1° × 1° grids. Note that only ensemble mean results of the two models for June–August from the integrations beginning at the end of February (and the forecast is completed in March) in each year are selected.

The monthly SST data are from the NOAA ERSST dataset, while the observed precipitation data are the standard monthly mean values from the CPC Merged Analysis of Precipitation (CMAP). The error (deviation) field of summer precipitation prediction is the difference between the model data and CMAP.

3. Decadal change characteristics in the EASP forecast

The spatial distributions of the EASP are revealed via empirical orthogonal function (EOF) analysis. The first EOF mode (EOF1) indicates the ocean–land difference with a variance contribution of 16.7% (Fig. 1a). The second EOF mode (EOF2) features

positive or negative anomalies alternately from north to south, with a variance contribution of 11.2% (Fig. 1b). The third EOF mode (EOF3) shows a "+ − +" pattern from north to south, with a variance contribution of 8.8%. EOF2 and EOF3 are consistent with the study by Huang et al. (2011) on the principal modes of summer precipitation in eastern China. Figures 1d–f show the time coefficients of EOF1, EOF2, and EOF3, respectively. It can be seen that EOF1 and EOF2 present mainly interannual oscillations, while EOF3 shows obvious decadal oscillation characteristics. The moving t-test (MTT) is used to identify the decadal adjustment of the time coefficients of the three EOF modes (Fig. 2). The abrupt change of the time coefficient of EOF3 occurring in 1999 passes the 95% confidence level, while there is no significant abrupt change information contained in the time coefficients of EOF1 and EOF2.

Figure 3a shows that the decadal change characteristics of the EASP anomalies are obvious, particularly along 30°–55°N where the "north-wet and south-dry" situation changed around 1999: before 1999, the north (40°–55°N) was wet, while the south (30°–40°N) was in drought, and then it became the opposite since

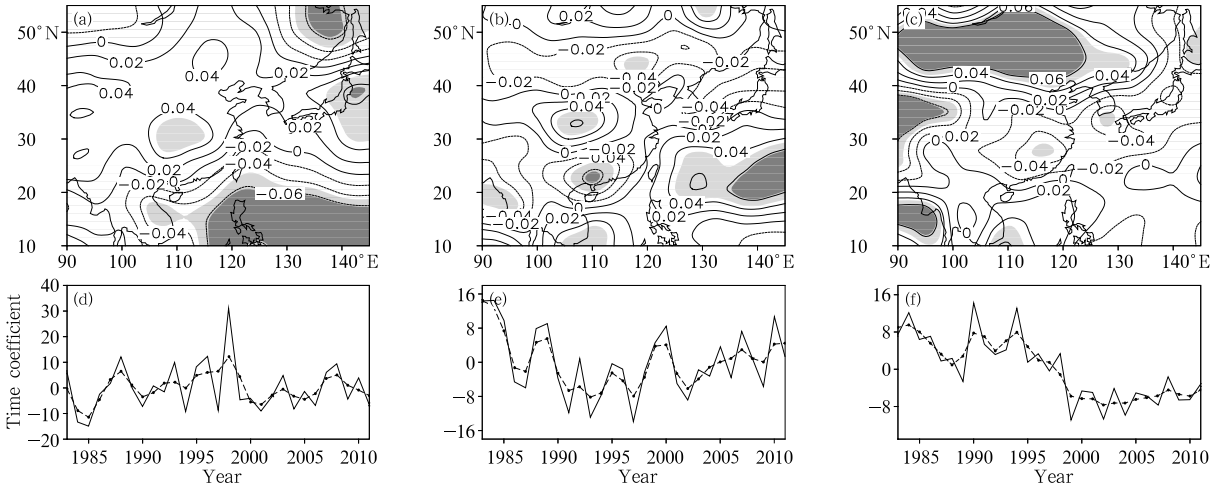

Fig. 1. (a–c) Spatial patterns of the EOF1, EOF2, and EOF3 of the EASP during 1983–2011 and (d–f) their corresponding time coefficients. The dark and grey shaded areas in (a–c) denote the 95% and 90% confidence levels respectively, and the dashed line with circles in (d–f) denotes the 9-point smoothing curve.

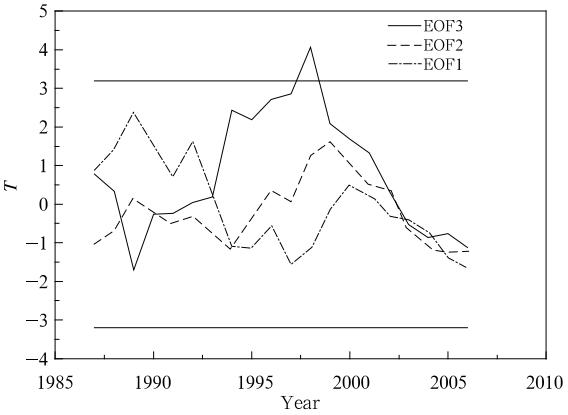

Fig. 2. Moving t-test of the time coefficient of EOF1, EOF2, and EOF3. The two parallel straight lines are the threshold values of the 95% confidence level.

1999. In Fig. 3b, less decadal change information is contained in the EASP hindcasts of BCC_CGCM; in particular, the "north-wet and south-dry" adjustment is not seen within 30°–55°N in 1999. In Fig. 3c, neither the drought nor the flood situation adjustment from north to south in 1999 is given by the EASP hindcasts of BCC_CSM.

Figure 4 shows the composite images of the EASP anomaly percentage in two intervals before and after 1999. Based on observations, the EASP anomaly percentage shows a "+ − +" pattern from north to south during 1983–1998, and an opposite anomalous pattern of "− + −" during 1999–2011 (Figs. $4a_1$ and $4b_1$). Meanwhile, the BCC_CGCM hindcasts produce a

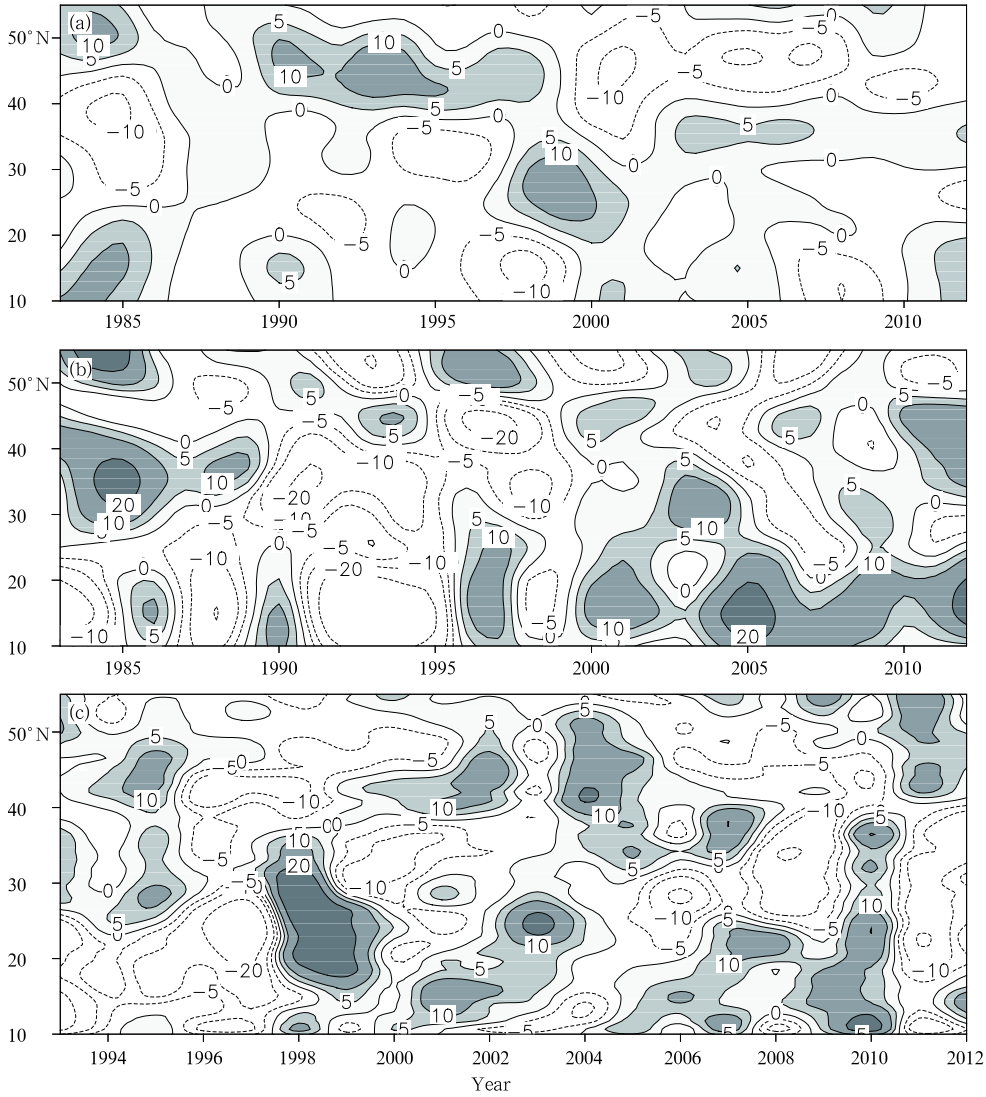

Fig. 3. Latitude–time section of the EASP anomaly percentage (%) along 90°–145°E, based on (a) CMAP (1983–2011), (b) BCC_CGCM (1983–2011), and (c) BCC_CSM (1991–2011). Solid and dashed lines denote positive and negative anomalies, respectively. Shadings denote positive anomalies.

"+ – + –" pattern from north to south during 1983–1998 and an opposite pattern of "– + – +" during 1999–2011 (Figs. $4a_2$ and $4b_2$), and the BCC_CSM hindcasts produce a "– + –" pattern from north to south during 1983–1998 and an opposite pattern of "+ – +" in 1999–2011 (Figs. $4a_3$ and $4b_3$). Therefore, the EASP hindcast results of BCC_CGCM and BCC_CSM contain decadal change information that deviates greatly from that observed.

4. SST decadal change characteristics

The decadal change characteristics of the SST around 1999 and the SST forecast abilities of BCC_CGCM and BCC_CSM are focused in this section. In Fig. 5, the time coefficient of EOF3 (TEOF3) of the EASP is significantly correlated with the summer SST, especially in West Pacific (20°S–20°N, 110°–116°E) and North Pacific (20°–50°N, 150°–180°E). As TEOF3 contains significant EASP decadal change characteristics, the SST, which is significantly correlated with TEOF3, may also have an influence on the EASP decadal adjustment in the late 1990s.

Figure 6 shows the SST anomaly in two periods (before and after 1999). Based on observations, North Pacific and West Pacific are controlled by negative

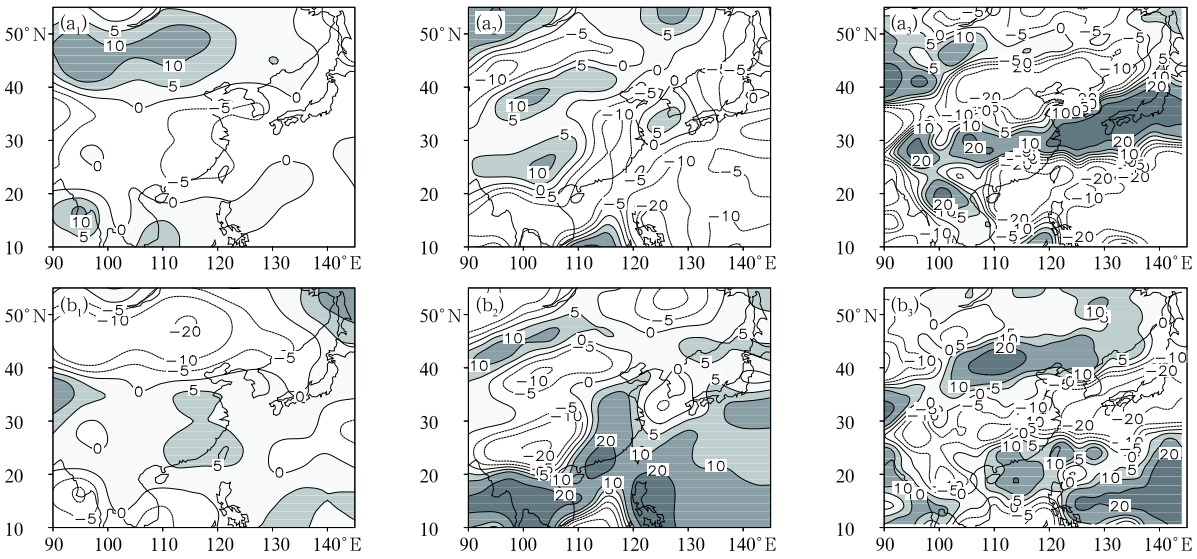

Fig. 4. Composites of the EASP anomaly percentage (%): (a_1, b_1) observations during 1983–1998 and 1999–2011, (a_2, b_2) as in (a_1, b_1), but for BCC_CGCM hindcasts, and (a_3, b_3) as in (a_1, b_1), but for BCC_CSM hindcasts. Solid and dashed lines denote positive and negative anomalies, respectively. Values in (a_2, b_2) are multiplied by 10, and in (a_3, b_3) by 5. Shadings denote positive anomalies.

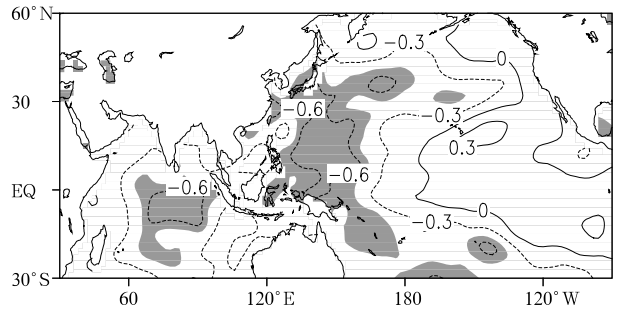

Fig. 5. Spatial distribution of ACCs between the time coefficients (TEOF3) of EASP and the summer SST anomalies for the period 1983–2011. Shaded areas correspond to the 95% confidence level.

SST during 1983–1998, and the equatorial and North Pacific SSTs present quasi-El Niño characteristics. During 1999–2011, North Pacific and West Pacific are both controlled by positive SST anomalies, while the equatorial and North Pacific SSTs show quasi-La Niña characteristics (Figs. $6a_1$ and $6b_1$). Based on the BCC_CGCM hindcasts, in the first period, North Pacific is dominated by warm SST and West Pacific by cold SST, and the equatorial SST anomalies show quasi-La Niña characteristics. In the second period, North Pacific is dominated by cold SST and West Pacific by warm SST, and the equatorial SST anomalies show quasi-El Niño characteristics (Figs. $6a_2$ and $6b_2$). Based on the BCC_CSM hindcasts, in the first period, North Pacific and West Pacific are both dominated by cold SST, and the equatorial SST anomalies show quasi-El Niño characteristics. In the second period, North Pacific and West Pacific are both dominated by warm SST, and the equatorial SST anomalies show quasi-La Niña characteristics (Figs. $6a_3$ and $6b_3$). Compared with observations, the BCC_CGCM hindcasts present opposite characteristics, while the BCC_CSM hindcasts show similar anomalies.

Figure 7 shows the annual SST anomaly average over West Pacific (SST1) and North Pacific (SST2). In observations, SST1 is dominated by negative values before the late 1990s, but then changes to positive values, with SST2 also showing a similar pattern of adjustment. Based on the BCC_CGCM hindcasts, SST1 is dominated by negative values in the first period, but then changes to positive values. SST2, meanwhile, presents obvious fluctuation, dominated by positive or close to normal SSTs in the first period, before changing to negative values. Based on the BCC_CSM hindcasts, SST1 and SST2 both show an adjustment from negative to positive values in the late 1990s.

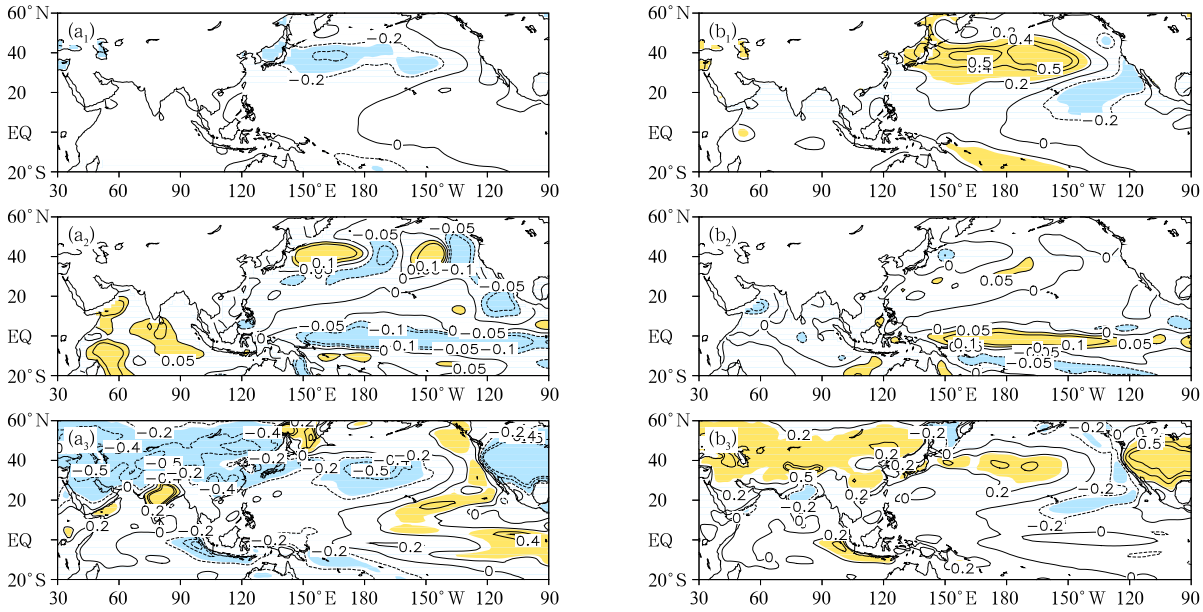

Fig. 6. Anomalous SST (℃) in summer for the periods (a_1–a_3) 1983–1998 and (b_1–b_3) 1999–2011, based on (a_1, b_1) observations, (a_2, b_2) BCC_CGCM, and (a_3, b_3) BCC_CSM. Yellow and blue areas correspond to the 90% confidence level.

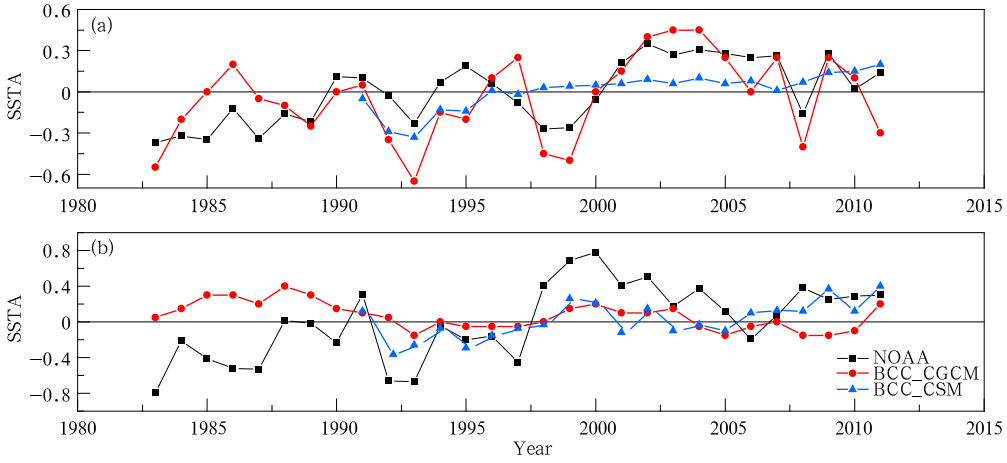

Fig. 7. Time series of annual SST anomaly (℃) averages. (a) SST1 over West Pacific (20°S–20°N, 110°E–116°E) and (b) SST2 over North Pacific (20°–50°N, 150°E–180°E).

Therefore, the warm–cold adjustment of these SST indices in the late 1990s in the BCC_CGCM hindcasts shows deviation from observations, while that of the BCC_CSM hindcasts is similar to observed.

5. Relationship between EASP and SST anomalies

In order to analyze the relationship between EASP and the SST anomaly, the distribution of ACCs is shown in Fig. 8. Based on observations, SST1 is negatively correlated with the precipitation of northern East Asia and positively correlated with that of the central and southern regions (Fig. 8a_1), while SST2 is negatively correlated with the precipitation of northern and central East Asia and positively correlated with that of local North China and southern East Asia (Fig. 8b_1). Based on BCC_CGCM, SST1

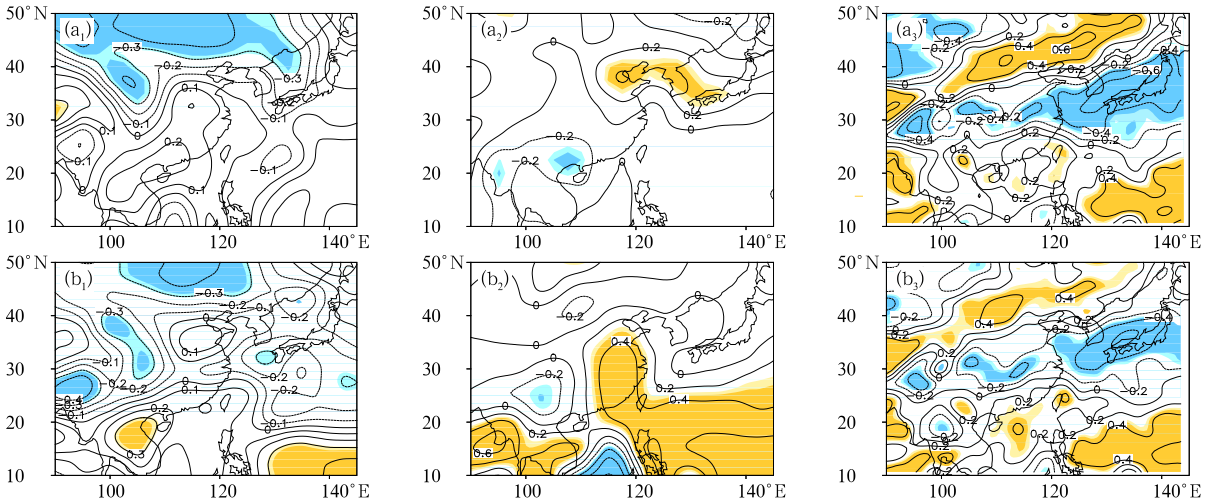

Fig. 8. Distributions of the ACCs between (a_1–a_3) SST1 and EASP and (b_1–b_3) SST2 and EASP, based on (a_1, b_1) observations, (a_2, b_2) BCC_CGCM hindcasts, and (a_3, b_3) BCC_CSM hindcasts. The dark blue and dark yellow shaded areas denote the 95% confidence level, and light blue and light yellow shaded areas denote the 90% confidence level.

is positively correlated with the precipitation over northern East Asia and negatively correlated with that over southern East Asia (Fig. $8a_2$), while SST2 is positively correlated with the precipitation over part of northern East Asia, southeastern China, and southern East Asia, and negatively correlated with that over the south of northern East Asia, southwestern China, as well as central and southern East Asia (Fig. $8b_2$). Based on BCC_CSM, SST1 and SST2 are both positively correlated with the precipitation over northern and southern East Asia, and significantly negatively correlated with the precipitation over central East Asia (Figs. $8a_3$ and $8b_3$). The distributions of positive and negative ACCs of BCC_CGCM and BCC_CSM, especially for locations of high-value centers, show obvious deviation from that of observations. This implies that the responses of EASP to the SST anomalies in BCC_CGCM and BCC_CSM themselves possess deviations, which in turn lead to the model hindcasts being unable to present the EASP decadal change.

Figure 9 shows the differences between the anomaly percentage composite of the precipitation in five high-value years (SST1: 1991, 1992, 1994, 1995, 1996; SST2: 1991, 1994, 1995, 1996, 1998) before 1999, corresponding to SST1 and SST2 in CMAP data, BCC_CGCM hindcasts, BCC_CSM hindcasts, and five high-value years (SST1: 2002, 2003, 2004, 2005, 2009; SST2: 1999, 2000, 2001, 2002, 2008) after 1999. In terms of the precipitation corresponding to high-SST1 years in the CMAP data, compared with the situation before and after 1999, the precipitation difference in northern East Asia, over the south-central peninsula and in some western areas, is significantly larger; while in central East Asia, parts of the West Pacific Ocean, and in coastal regions, it is less. In terms of high-SST2 years, the precipitation difference before and after 1999 is similar to that of SST1 (Figs. $9a_1$ and $9b_1$). In BCC_CGCM, the variability of precipitation anomaly percentage is significantly lower than observed. For high-SST1 years, compared with the situation before and after 1999, the anomaly percentage distribution of precipitation difference in West Pacific is similar to observed, but opposite to the situation over land. For high-SST2 years, the difference of precipitation anomaly percentage over land shows large deviation from that based on observations (Figs. $9a_2$ and $9b_2$). In BCC_CSM, the variability of precipitation anomaly percentage is obviously lower than observed. In terms of spatial distribution, the precipitation anomaly percentage difference distribution over the tropical and subtropical West Pacific is similar to that based on observations, but significant deviation exists for most of East Asia, particularly northern East Asia (Figs. $9a_3$ and $9b_3$).

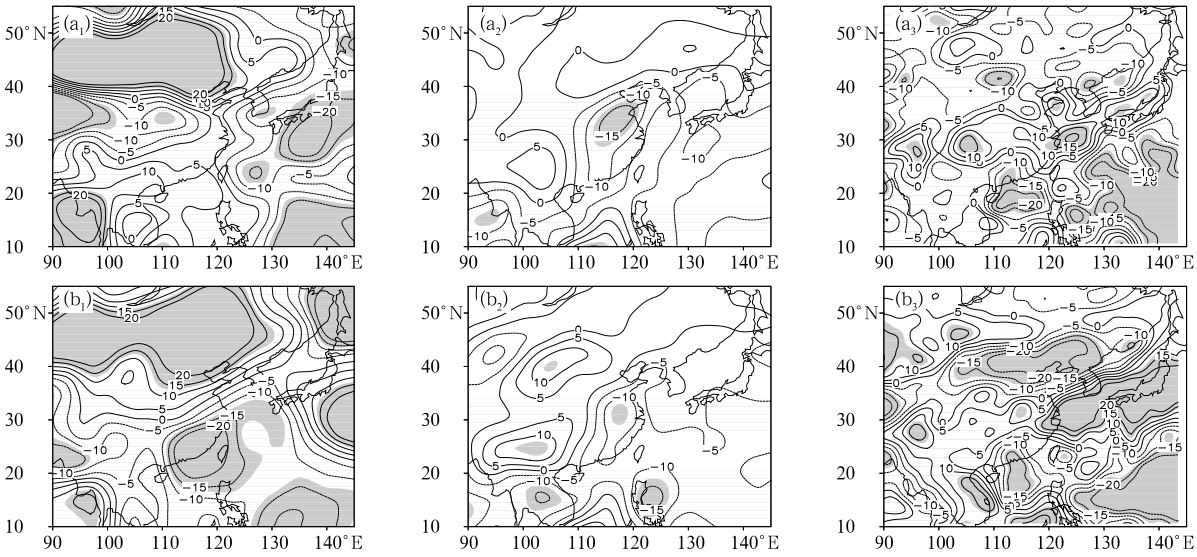

Fig. 9. Differences of anomaly percentage (%) composition of summer precipitation in five high-value years, corresponding to (a_1–a_3) SST1 and (b_1–b_3) SST2, respectively, in (a_1, b_1) CMAP, (a_2, b_2) BCC_CGCM, and (a_3, b_3) BCC_CSM, between periods before and after 1999. Values of the contours in (a_2, b_2, a_3, and b_3) are all doubled. Shaded areas denote the 90% confidence level.

Therefore, considerable deviation is apparent in BCC_CGSM and BCC_CSM regarding the distribution of ACCs, as well as the spatial distribution of the precipitation anomaly percentage, corresponding to high-value SST years before and after 1999, which may together lead to the model hindcasts failing to reflect the decadal adjustment of EASP around 1999.

6. Dynamic–analogue correction of the EASP decadal change in the late 1990s

The above analysis shows that both the BCC_CGCM and BCC_CSM hindcasts fail to produce the decadal adjustment of the EASP that took place in the late 1990s. The reasons for this might be: (1) the warm–cold adjustment of the SST in the late 1990s in the BCC_CGCM hindcasts deviates considerably from observations, and (2) the response of EASP to the SST anomalies in both BCC_CGCM and BCC_CSM hindcasts demonstrates certain deviation. Based on SST1, SST2, and SST3 (average of SST1 and SST2), an EASP dynamic–analogue forecast scheme is presented in Fig. 10. The main technical steps involved can be summarized as follows:

(1) Obtain the forecast errors of the models for EASP based on CMAP precipitation field, and the forecast fields of BCC_CGCM (BCC_CSM) in past years. Conduct EOF decomposition on the EASP and determine the EOF components that contain the key characteristics of decadal variation of EASP and their corresponding time coefficients.

(2) Calculate the ACCs between the time coefficients of the EOF components and the global SST field, and determine the significantly correlated key sea areas. Analyze the correlation between the key SST areas and the EASP forecast errors. The better the correlation is, the more likely the area can be used for the selection of historically similar error information.

(3) Based on the SST average time series of the key areas that are correlated well with the EASP forecast errors, select the historical years most similar to the SST status of the current case, and then as extract the EASP forecast errors of BCC_CGCM (BCC_CSM) for these similar years.

(4) Combine the extracted historically similar errors composite with the EASP forecast result provided by BCC_CGCM (BCC_CSM) for the summer of the current year, and obtain the corrected forecast results.

Figure 11 shows the corrected latitude-time sec-

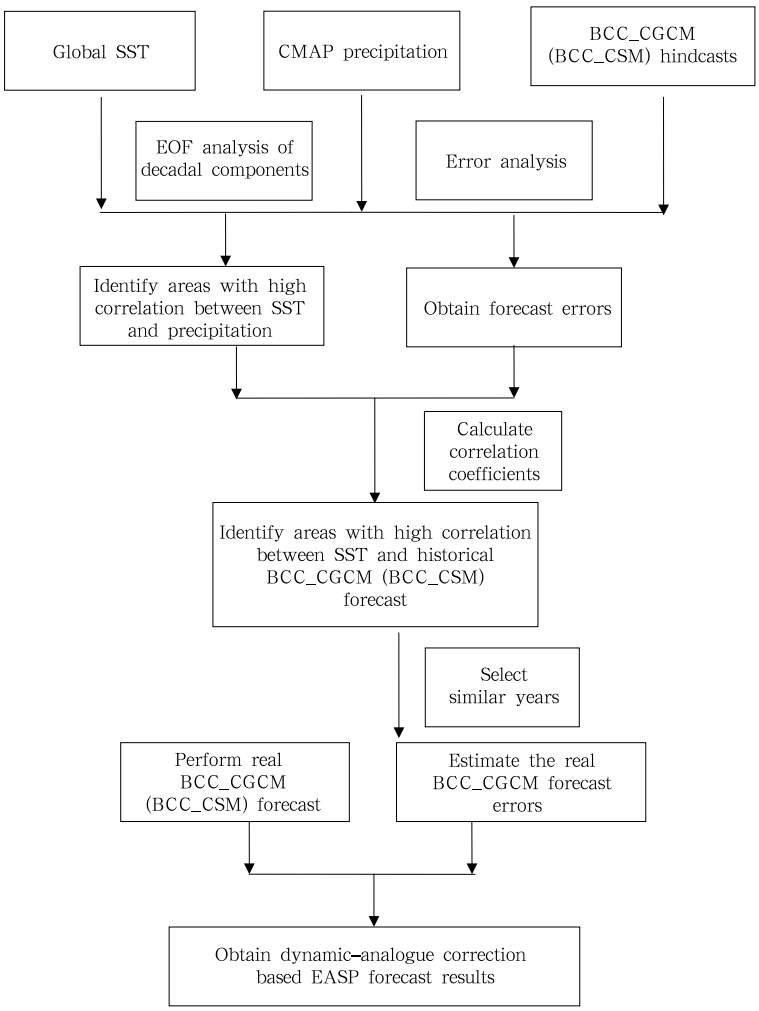

Fig. 10. Flow diagram of the dynamic–analogue correction scheme for the EASP forecast based on the decadal change information.

tion of the precipitation anomaly percentage. Table 1 shows that, for the BCC_CGCM hindcasts before correction, the ACC of EASP anomaly percentage is –0.01 within 30°–55°N. However, the SST1-based corrected BCC_CGCM hindcasts of EASP show a "+ – +" pattern from north to south before 1999, but a change of pattern to "– + –" after 1999. The decadal adjustment in northern East Asia is particularly evident (Fig. 11a$_1$), close to observations. The ACC of the precipitation anomaly percentage in the section is 0.16. The SST2-based correction of precipitation in the BCC_CGCM hindcasts also shows a clear decadal adjustment in northern East Asia around 1999 (Fig. 11a$_2$), and the ACC within 30°–55°N is 0.11. Based on SST3, the corrected EASP shows a "+ – +" pattern before 1999 and an opposite pattern after 1999 (Fig. 11a$_3$), with the ACC within 30°–55°N being 0.13. Considering the correction based on both SST1 and SST2, the average is also calculated, which is also very close to observations (Fig. 11a$_4$), with an ACC of 0.18. Therefore, both the ACC and distribution of the latitude-time section of the EASP are significantly improved compared with the BCC_CGCM hindcasts before correction.

Table 1 shows the ACC of the EASP anomaly percentage to be –0.09 for the BCC_CSM hindcasts before correction. However, the SST1-based corrected BCC_CSM hindcasts reflect the decadal adjustment of EASP in northern East Asia around 1999 (Fig. 11b$_1$), while the SST2-based correction is not as good

(Fig. 11b$_2$). The ACCs of the SST1 and SST2 corrected values are –0.05 and –0.02, respectively. Both are somewhat better than the situation before correction. Based on SST3, the corrected EASP shows a "+ – +" pattern before 1999 and an opposite pattern after 1999 (Fig. 11b$_3$), and the ACC within 30°–55°N is 0.11. For the average of SST1- and SST2-based corrections (Fig. 11b$_4$), the ACC within 30°–55°N is 0.02. Therefore, both the ACC and spatial distribution of the corrected latitude-time section of the EASP are somewhat improved, compared with the BCC_CCM hindcasts before correction.

The ACCs between the EASP mean of observations and the mean of BCC_CGCM hindcasts during 1983–1998 and 1999–2011 are shown in Table 2. It is clear that the ACCs after correction, especially those of SST1- and SST2-based corrections, with ACCs of 0.85 and 0.76, respectively, are much better than those before correction. The ACCs between the EASP mean of observations and the mean of BCC_CSM hindcasts during 1991–1998 and 1999–2011 are also shown in Table 2. The ACCs of the SST1- and SST2-based corrections are 0.79 and 0.78, which are also much better than those before correction.

Table 1. ACCs of the latitude-time section of the EASP anomaly percentage between independent sample validation and CMAP

Model	Before correction	SST1	SST2	SST3	Mean
BCC_CGCM (1983–2011)	–0.01	0.11*	0.16**	0.13	0.18**
BCC_CSM (1991–2011)	–0.09	–0.05	–0.02	0.11	0.02

Note: * 90% confidence level, ** 95% confidence level. Mean indicates the average of SST1- and SST2-based corrections.

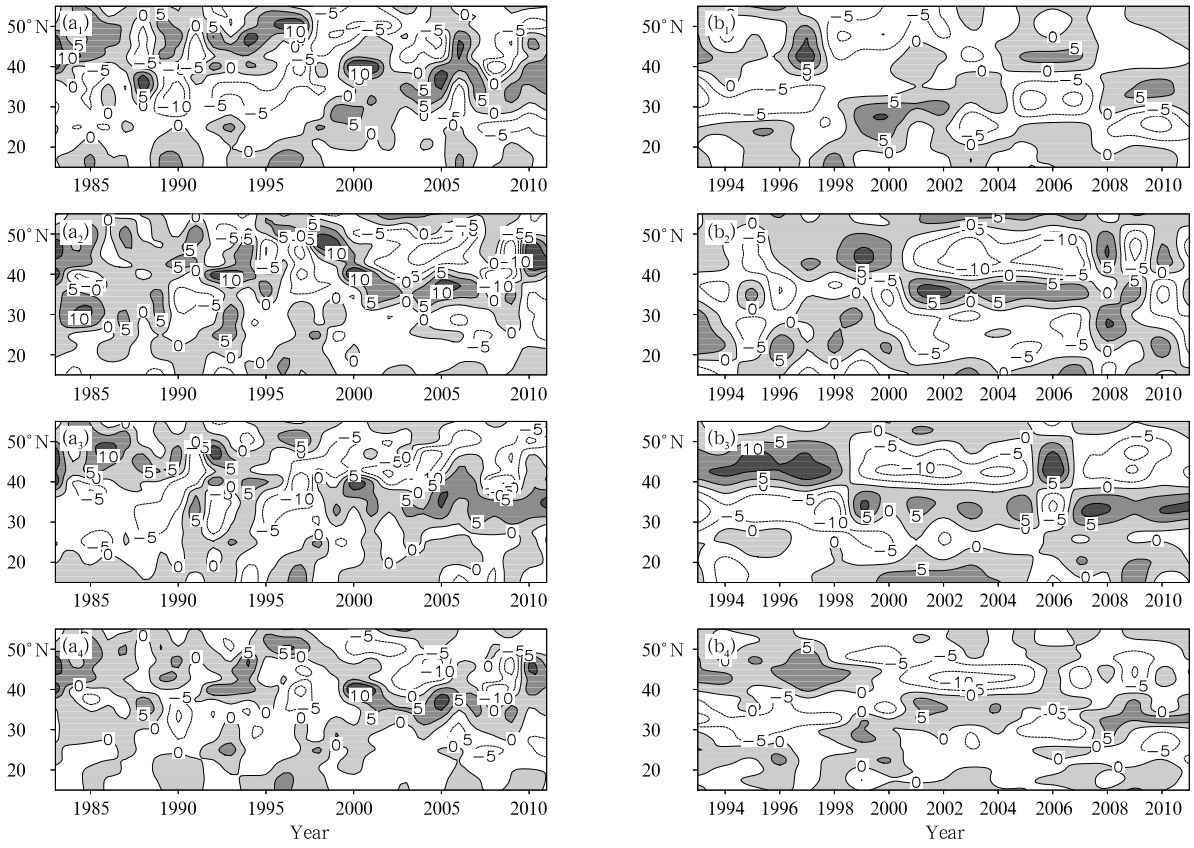

Fig. 11. Latitude–time sections of the EASP anomaly percentage (%) along 90°–145°E: (a$_1$, b$_1$) SST1-based correction; (a$_2$, b$_2$) SST2-based correction; (a$_3$, b$_3$) SST3-based correction; (a$_4$, b$_4$) the mean of SST1- and SST2-based correction. Solid and dashed lines denote positive and negative anomalies, respectively. Shadings denote positive anomalies.

Table 2. ACCs of the mean precipitation anomaly between observations and model hindcasts

Model	BCC_CGCM		BCC_CSM	
Period	1983–1998	1999–2011	1991–1998	1999–2011
Before correction	0.03	0.08	0.17*	0.17*
SST1-based correction	0.76*	0.44*	0.37*	0.09
SST2-based correction	0.42*	0.57*	0.08*	0.60*
SST3-based correction	0.85*	0.76*	0.79*	0.78*
Mean	0.81*	0.59*	0.33*	0.55*

Note: * 90% confidence level. Mean indicates the average of SST1- and SST2-based corrections.

7. Conclusions and discussion

Based on two coupled global models, BCC_CGCM and BCC_CSM, the EASP decadal change information in the late 1990s contained within the models' precipitation hindcasts are evaluated in this paper. The reasons behind the deviations in the decadal change in the BCC_CGCM and BCC_CSM hindcasts from the observations are analyzed. A new dynamic-analogue correction scheme is then proposed to improve the decadal change information in the models' seasonal predictions. The preliminary findings can be summarized as follows.

In the BCC_CGCM and in BCC_CSM hindcasts, the decadal change in the EASP around the late 1990s shows a certain deviation from the observation. Before correction, in BCC_CGCM, the ACC within 30°–55°N of the EASP anomaly percentage between hindcasts and observations is –0.01, and in BCC_CSM it is –0.09. After correction, in BCC_CGCM, the average ACC of the EASP anomaly is 0.03 and 0.08 for the periods 1983–1998 and 1999–2011, respectively; while in BCC_CSM, the ACCs are both 0.17.

Evident deviations from observations are also found in the BCC_CGCM and BCC_CSM hindcasts for the North Pacific and West Pacific SSTs, with the following features. (1) The spatial distribution of SST anomalies and annual evolution of SST1 and SST2 in the BCC_CGCM hindcasts show opposite characteristics to observations, while the hindcasts of BCC_CSM are closer to observations. (2) The locations of high-value centers of ACCs between the time series of the average SST anomaly and EASP in both models are quite different from those in observations. For years with high-value SST1 and SST2 before and after 1999, the spatial distribution of composite precipitation difference of BCC_CGSM and BCC_CSM hindcasts both present obvious deviations from observastions. Therefore, the SST forecast errors and deviations and the subsequent EASP response to the SST anomalies in BCC_CGCM and BCC_CSM may together lead to the models failing to reflect the decadal adjustment of the EASP around 1999.

Based on the evaluation and attribution of the deviations in the decadal adjustment of the EASP in the late 1990s in the BCC_CGCM and BCC_CSM hindcasts, a dynamic–analogue correction scheme is proposed. The scheme is then employed to improve the EASP decadal change information in the model hindcasts. The corrected results indicate that the decadal spatial distribution pattern of the EASP anomalies before and after 1999 are both obviously improved. For SST1-, SST2-, and SST3-based corrections, the ACCs of the latitude-time section (30°–50°N) of the EASP are improved from –0.01 to 0.11, 0.16, and 0.13 for BCC_CGCM, and from –0.09 to –0.02, –0.05, and 0.11 for BCC_CSM, respectively. Note that the improved ACCs, especially those of BCC_CSM, are still very low, even after correction. The reasons for this might be that (1) the precipitation prediction skill of the two models is low, making it more difficult to achieve highly improved ACCs; and (2) the EASP evolution contains not only a decadal signal, but also annual variability; the dynamic–analogue correction scheme used in this study focuses mainly on improving the decadal adjustment, and thus has a limited effect on improving the total variability of EASP. However, it is also shown in Table 2 that the EASP decadal change information around 1999 contained within the two models can be effectively improved by using the dynamic–analogue correction scheme. Specifically, the ACCs of the average precipitation anomalies in BCC_

CGCM/BCC_CSM before and after 1999 are significantly improved from 0.03/0.17 and 0.08/0.17 to 0.81/0.33 and 0.59/0.55.

It is inferred that the reasons why our newly proposed scheme is able to improve the decadal change information contained within the model output might be that: (1) the existence of the PDO, AMO, and other abnormal modes in the SST field may have important influences on the East Asian monsoon system and associated summer precipitation (Huang et al., 2011); (2) one of the important premises for a model to correctly predict EASP is that the model can well predict SST anomalies, and the atmosphere responds decently to the external forces of SST in some key areas. Otherwise, an initial deviation of SST may result in a precipitation prediction error in the dynamic prediction result (Chou, 1986); (3) therefore, when deviations occur in the model prediction in SST key areas, it is possible to obtain similar historical information in model precipitation hindcasts by considering the analogues existing in the time series of the SST key areas; and (4) then, similar historical information selected can be used to correct the model precipitation prediction deviations (Lang and Wang, 2010).

REFERENCES

Bond, N. A., and D. E. Harrison, 2000: The Pacific decadal oscillation, air–sea interaction and central North Pacific winter atmospheric regimes. *Geophys. Res. Lett.*, **27**, 731–734, doi: 10.1029/1999GL010847.

Chen, L. X., M. Dong, and Y. N. Shao, 1992: The characteristics of interannual variations on the East Asian monsoon. *J. Meteor. Soc. Japan*, **70**, 397–421.

Chou Jifan, 1974: A problem of using past data in numerical weather forecasting. *Sci. China (Ser. A)*, **17**, 814–825. (in Chinese)

Chou Jifan, 1986: Why to combine dynamical and statistical methods together and how to combine. *Plateau Meteor.*, **5**, 367–372. (in Chinese)

Ding, Y. H., 1992: Summer monsoon rainfalls in China. *J. Meteor. Soc. Japan*, **70**, 373–396.

Ding Yihui, Liu Yiming, Song Yongjia, et al., 2002: Research and experiments of the dynamical model system for short-term climate prediction. *Clim. Environ. Res.*, **7**, 236–246. (in Chinese)

Ding, Y. H., Z. Y. Wang, and Y. Sun, 2008: Interdecadal variation of the summer precipitation in East China and its association with decreasing Asian summer monsoon. Part I: Observed evidences. *Int. J. Climatol.*, **28**, 1139–1161, doi: 10.1002/joc.1615.

Enfield, D. B., A. M. Mestas-Nuñez, and P. J. Trimble, 2001: The Atlantic multidecadal oscillation and its relation to rainfall and river flows in the continental U.S. *Geophys. Res. Lett.*, **28**, 2077–2080, doi: 10.1029/2000GL012745.

Fan Ke, Wang Huijun, and Choi Young-Jean, 2007: A physical and statistical prediction model for summer precipitation over the lower reaches of Yangtze River. *Chin. Sci. Bull.*, **52**, 2900–2905.

Feng Guolin, Cao Hongxing, Gao Xinquan, et al., 2001: Prediction of precipitation during summer monsoon with self-memorial model. *Adv. Atmos. Sci.*, **18**, 701–709.

Feng Guolin, Zhao Junhu, Zhi Rong, et al., 2013: Recent progress on the objective and quantifiable forecast of summer precipitation based on dynamical statistical method. *J. Appl. Meteor. Sci.*, **24**, 656–665. (in Chinese)

Gershunov, A., and T. P. Barnett, 1998: Interdecadal modulation of ENSO teleconnections. *Bull. Amer. Meteor. Soc.*, **79**, 2715–2725, doi: 10.1175/1520-0477(1998)079<2715:IMOET>2.0.CO;2.

Gong Zhiqiang, Hou Wei, and Feng Guolin, 2012: Study of tropical middle–eastern Pacific sea surface temperature correlation index and probable correlation with ENSO effects. *Acta Meteor. Sinica*, **70**, 1074–1083. (in Chinese)

Gong Zhiqiang, Zhao Junhu, and Feng Guolin, 2013: Analysis of the summer precipitation of 2012 in East China and its possibility of decadal shift. *Acta Phys. Sinica*, **62**, 099205. (in Chinese)

Gong, Z. Q., J. H. Zhao, G. L. Feng, et al., 2015: Dynamic-statistics combined forecast scheme based on the abrupt decadal change component of summer precipitation in East Asia. *Sci. China (Ser. D)*, **58**, 404–419, doi: 10.1007/s11430-014-4967-4.

He, W. P., G. L. Feng, Q. Wu, et al., 2012: A new method for abrupt dynamic change detection of correlated time series. *Int. J. Climatol.*, **32**, 1604–1614, doi: 10.1002/joc.2367.

Huang Gang and Yan Zhongwei, 1999: The East Asian summer monsoon circulation anomaly index and its interannual variations. *Chin. Sci. Bull.*, **44**, 1325–1329.

Huang, J. P., Y. H. Yi, S. W. Wang, et al., 1993: An analogue–dynamical long-range numerical weather prediction system incorporating historical evolution. *Quart. J. Roy. Meteor. Soc.*, **119**, 547–565.

Huang, J. P., K. Higuchi, and A. Shabbar, 1998: The relationship between the North Atlantic Oscillation and El Niño–Southern Oscillation. *Geophys. Res. Lett.*, **25**, 2707–2710.

Huang Ronghui, Chen Jilong, and Liu Yong, 2011: Interdecadal variation of the leading modes of summertime precipitation anomalies over eastern China and its association with water vapor transport over East Asia. *Chinese J. Atmos. Sci.*, **35**, 589–606. (in Chinese)

Keenlyside, N. S., M. Latif, J. Jungclaus, et al., 2008: Advancing decadal-scale climate prediction in the North Atlantic sector. *Nature*, **453**, 84–88, doi: 10.1038/nature06921.

Kim, H. M., P. J. Webster, and J. A. Curry, 2012: Evaluation of short-term climate change prediction in multi-model CMIP5 decadal hindcasts. *Geophys. Res. Lett.*, **39**, L10701, doi: 10.1029/2012GL051644.

Lang, X. M., and H. J. Wang, 2010: Improving extra seasonal summer rainfall prediction by merging information from GCMs and observations. *Wea. Forecasting*, **25**, 1263–1274, doi: 10.1175/2010WAF2222342.1.

Li Weijing, Zhang Peiqun, Li Qingquan, et al., 2005: Research and operational application of dynamical climate model prediction system. *J. Appl. Meteor. Sci.*, **16**, 1–11. (in Chinese)

Lian Yi, Shen Baizhu, Gao Zongting, et al., 2003: The study of the onset criterion and the date of East Asian summer monsoon in Northeast China and its main characteristic analysis. *Acta Meteor. Sinica*, **61**, 548–558. (in Chinese)

Lian Yi, Shen Baizhu, and Gao Zongting, 2004: An exploration on the determination of East Asian summer monsoon index. *Acta Meteor. Sinica*, **62**, 782–789. (in Chinese)

Ma Zhuguo and Fu Congbin, 2007: Evidences of drying trend in the global during the latter half of 20th century and their relationship with large-scale climate background. *Sci. China (Ser. D)*, **37**, 222–233.

Smith, D. M., S. Cusack, A. W. Colman, et al., 2007: Improved surface temperature prediction for the coming decade from a global climate model. *Science*, **317**, 796–799, doi: 10.1126/science.1139540.

Smith, D. M., A. A. Scaife, G. J. Boer, et al., 2013: Real-time multi-model decadal climate predictions. *Climate Dyn.*, **41**, 2875–2888, doi: 10.1007/s00382-012-1600-0.

Wang Huijun, 2001: The weakening of the Asian monsoon circulation after the end of 1970s. *Adv. Atmos. Sci.*, **18**, 376–386.

Wang, L., W. Chen, and R. H. Huang, 2008: Interdecadal modulation of PDO on the impact of ENSO on the East Asian winter monsoon. *Geophys. Res. Lett.*, **35**, L20702, doi: 10.1029/2008GL035287.

Wang Qiguang, Feng Guolin, Zheng Zhihai, et al., 2011: A study of the objective and quantifiable forecasting based on optimal factors combinations in precipitation in the middle and lower reaches of the Yangtze River in summer. *Scientia Atmospherica Sinica*, **35**, 287–297. (in Chinese)

Wang Xiaojuan, Zhi Rong, He Wenping, et al., 2012: Collective behaviour of climate indices in the North Pacific air–sea system and its potential relationships with decadal climate changes. *Chin. Phys. B*, **21**, 029201, doi: 10.1088/1674-1056/21/2/029201.

Wu, R. G., Z. Z. Hu, and B. P. Kirtman, 2003: Evolution of ENSO-related rainfall anomalies in East Asia. *J. Climate*, **16**, 3742–3758, doi: 10.1175/1520-0442(2003)016<3742:EOERAI>2.0.CO;2.

Wu Tongwen, Song Lianchun, Liu Xiangwen, et al., 2013: Progress in developing the short-range operational climate prediction system of China National Climate Center. *Quart. J. Appl. Meteor.*, **24**, 533–543. (in Chinese)

Xu, H. L., J. Feng, and C. Sun, 2013: Impact of preceding summer North Atlantic oscillation on early Autumn precipitation over central China. *Atmos. Oceanic Sci. Lett.*, **6**, 417–422.

Xu, Z. Q., K. Fan, and H. J. Wang, 2015: Decadal variation of summer precipitation over China and associated atmospheric circulation after the late 1990s. *J. Climate*, **28**, 4086–4106, doi: 10.1175/JCLI-D-14-00464.1.

Yang Jie, Zhao Junhu, Zheng Zhihai, et al., 2012: Estimating the prediction errors of dynamical climate model on the basis of prophase key factors in North China. *Chinese J. Atmos. Sci.*, **36**, 11–22. (in Chinese)

Yang Xiuqun, Xie Qian, Zhu Yimin, et al., 2005: Decadal-to-interdecadal variability of precipitation in North China and associated atmospheric and oceanic anomaly patterns. *Chinese J. Geophys.*, **48**, 789–797. (in Chinese)

Zheng Zhihai, Ren Hongli, and Huang Jianping, 2009: Analogue correction of errors based on seasonal climatic predictable components and numerical experiments. *Acta Phys. Sinica*, **58**, 7359–7367. (in Chinese)

Zhou, T. J., R. C. Yu, J. Zhang, et al., 2009: Why the western Pacific subtropical high has extended westward since the late 1970s. *J. Climate*, **22**, 2199–2215, doi: 10.1175/2008JCLI2527.1.